Template-Assisted Formation of Rattle-type V_2O_5 Hollow Microspheres with Enhanced Lithium Storage Properties

Hao Bin Wu, Anqiang Pan, Huey Hoon Hng, and Xiong Wen (David) Lou**

In this work, rattle-type ball-in-ball V_2O_5 hollow microspheres are controllably synthesized with the assistance of carbon colloidal spheres as hard templates. Carbon spheres@vanadium-precursor (CS@V) core–shell composite microspheres are first prepared through a one-step solvothermal method. The composition of solvent for the solvothermal synthesis has great influence on the morphology and structure of the vanadium-precursor shells. V_2O_5 hollow microspheres with various shell architectures can be obtained after removing the carbon microspheres by calcination in air. Moreover, the interior hollow shell can be tailored by varying the temperature ramping rate and calcination temperature. The rattle-type V_2O_5 hollow microspheres are evaluated as a cathode material for lithium-ion batteries, which manifest high specific discharge capacity, good cycling stability and rate capability.

1. Introduction

Hollow micro-/nano-structured metal oxides have attracted great interests because of their unique structure-determined physical and chemical properties that make them promising materials in a wide range of applications,[1–5] such as drug delivery,[6,7] photocatalysis,[8,9] dye-sensitized solar cells,[10,11] gas sensors[12,13] and lithium-ion batteries (LIBs).[14,15] Although great efforts have been dedicated to template-free routes for the preparation of hollow particles,[15–17] templating against colloidal particles is still the most effective and general method for the preparation of hollow particles with a narrow size distribution and well-defined shape.[18,19] It requires the controlled construction of desirable functional structure upon the template particles. Among the colloidal templates, monodisperse polymer latex, carbon, and silica spheres are commonly used because they are readily available in a wide range of sizes.[20,21] The common difficulties in template-based synthesis arise from creating uniform coatings of desired materials (or their precursors) on the surface of templates and maintaining their structural integrity after removing templates. Moreover, controllable preparation of hollow particles with complex architectures, such as multi-shell or yolk-shell structures, via a simple templating process still remains difficult.

As a transition metal oxide, vanadium pentoxide (V_2O_5) with a layered structure has been extensively studied as high capacity cathode materials for LIBs in the past decades.[21–25] However, its limited long-term cycling stability has been the major issue that prevents their practical use, which arises from its poor structural stability, low conductivity and slow electrochemical kinetics.[26,27] Recently, porous or hollow structured V_2O_5 materials have drawn particular interest because of their structural advantages for facile Li^+ ions insertion and good cycling stability.[22,28–31] However, the controllable synthesis of uniform V_2O_5 hollow structures with tunable shell structures still remains as a big challenge. Although templating against colloidal particles is straight-forward, the preparation of V_2O_5 hollow microspheres by templating methods is rarely reported.[32,33] This might arise from the compatibility issue between the shell material and the template. Additionally, the special chemical stability of V_2O_5, which can be dissolved in both alkaline and acid solutions, might introduce extra difficulty in the template removal process, such as for silica template. Therefore, carbonaceous or polymer spheres that can be removed by a calcination process are favorable as the supporting templates for the growth of vanadium oxide or its precursor shell.

Herein, we report the controllable synthesis of novel rattle-type V_2O_5 hollow microspheres with the assistance of carbon colloidal spheres as hard templates. Carbon spheres@vanadium-precursor (CS@V) core–shell composite microspheres are first prepared through a one-step solvothermal method. The composition of solvent for the solvothermal synthesis has great influence on the morphology and structure of the vanadium-precursor shells. V_2O_5 hollow microspheres with various shell architectures can be obtained after removing the carbon microspheres by calcination in air. Moreover, the interior hollow shell can be tailored by varying the temperature ramping rate and calcination temperature. When evaluated as a cathode material for LIBs, the rattle-type V_2O_5 hollow microspheres exhibit superior cycling stability and rate capability.

H. B. Wu, Dr. A. Q. Pan, Prof. X. W. Lou
School of Chemical & Biomedical Engineering
Nanyang Technological University
62 Nanyang Drive, 637459, Singapore
E-mail: pananqiang@gmail.com; xwlou@ntu.edu.sg
H. B. Wu, Prof. H. H. Hng
School of Materials Science and Engineering
Nanyang Technological University
50 Nanyang Avenue, 639798, Singapore
Dr. A. Q. Pan
School of Materials Science & Engineering
Central South University
Hunan, 410083, China

DOI: 10.1002/adfm.201300976

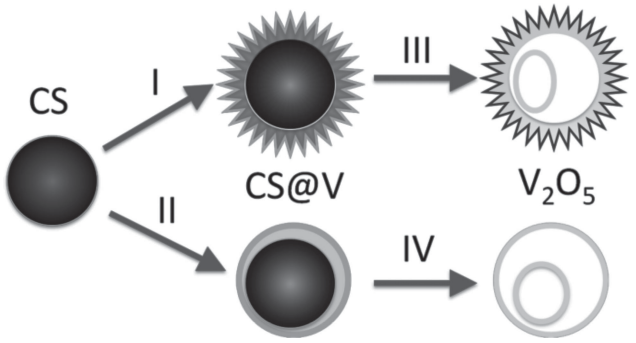

Figure 1. Schematic illustration of the preparation of carbon sphere@vanadium-precursor (CS@V) core–shell composite microspheres and their conversion to rattle-type V_2O_5 hollow microspheres. Step I and II represent the solvothermal synthesis of CS@V composite microspheres using different solvents. Step III and IV represent their transformation to V_2O_5 hollow microspheres by calcination in air.

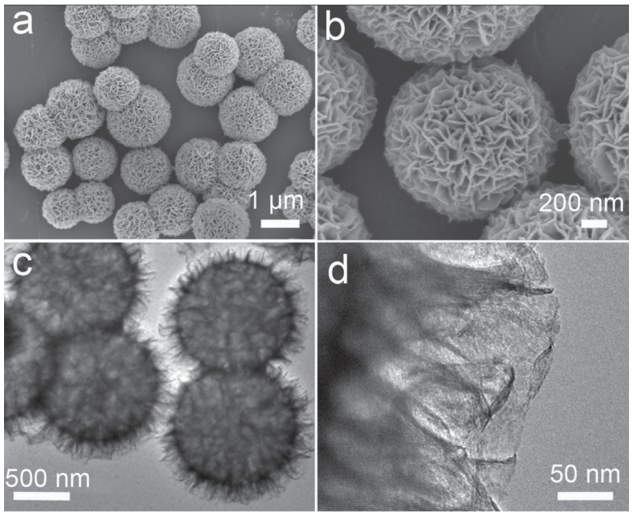

Figure 2. a,b) FESEM and c,d) TEM images of the solvothermally prepared CS@V-I core–shell composite microspheres using IPA as the solvent.

2. Results and Discussion

The high quality colloidal carbon spheres are firstly synthesized through a simple hydrothermal method using glucose as the carbon source.[34] The carbon spheres are highly uniform with a mean size of 0.8 μm (Figure S1, Supporting Information). In view of the large amount of hydrophilic functional groups on the surface and the easy removal via calcination, these carbon spheres are very attractive as hard templates for the fabrication of hollow particles.[34,35] The synthesis of rattle-type V_2O_5 hollow microspheres with the assistance of carbon spheres as the hard templates is schematically illustrated in **Figure 1**. As indicated by step I and II, vanadium-precursor shells with different morphology could be grown on the carbon spheres depending on the used solvent, thus forming the CS@V core–shell composite microspheres. After annealing the CS@V microspheres in air (step III and IV), their corresponding V_2O_5 hollow microspheres can be obtained. The exterior shell remains intact after the annealing process. Furthermore, under controlled annealing conditions, rattle-type (or ball-in-ball) hollow structures can be produced.

Figure 2 shows the solvothermally prepared hierarchical CS@V composite microspheres as indicated by step I in Figure 1 (denoted as CS@V-I microspheres). Isopropanol (IPA) is exclusively used as the solvent for the solvothermal reaction. As depicted in Figure 2a, it is evident that the vanadium-precursor has been uniformly grown on the carbon spheres in the form of densely assembled nanosheets. The growth of the vanadium-precursor shell also leads to the interconnection of some microspheres. No bare carbon spheres or unsupported nanosheets are found in the product, suggesting the good compatibility between the vanadium-precursor and the surface of templates. The enlarged field-emission scanning electron microscope (FESEM) image (Figure 2b) reveals more detailed features of the vanadium-precursor shell, which is composed of small interconnected nanosheets with small thickness of around 10 nm. The transmission electron microscope (TEM) image shown in Figure 2c clearly demonstrates the core–shell structure of the CS@V-I microspheres. The nanosheets are closely attached on the surface of the carbon spheres, and serve as the building blocks to construct the hierarchical shell with a thickness of around 200 nm. The magnified TEM image (Figure 2d) reveals the curved and flexible texture of the thin nanosheets. X-ray powder diffraction (XRD) pattern of the CS@V-I microspheres (Figure S2, Supporting Information) shows no detectable diffraction peaks, indicating the amorphous nature of the vanadium-precursor layer.

Slight variation of the solvent would result in different structures and crystal phases of the composite microspheres. As indicated in step II of Figure 1, yolk-shell CS@V microspheres (denoted as CS@V-II microspheres) can be produced by adding 2 mL of de-ionized (DI) water into the solution for the synthesis of CS@V-I microspheres, while keeping other parameters unaltered. The crystallographic structure of as-obtained CS@V-II microspheres is determined by XRD to be the recently reported VO_2 phase (Figure S2, Supporting Information).[31] A panoramic view (**Figure 3**a) shows that the sample consists of discrete microspheres of around 1 μm with very rough surface. The enlarged FESEM image (Figure 3b) of a broken microsphere reveals the yolk-shell structure, which is a unique class of core–shell structure with a distinct void space between the shell and the core. The shell of the CS@V-II microspheres is composed of loosely packed nanoparticles with a size of about 20 nm. In addition, a relatively smooth core is observed inside the microsphere with an obvious gap from the exterior shell. The yolk-shell structure is further confirmed by TEM observation (Figure 3c,d). The low contrast of the core suggests that it is likely the carbon sphere template, while some V-based species might also exist on the surface. The thickness of the porous shell is estimated to be around 100 nm, with a gap of about 200 nm apart from the exterior shell. The formation of such a yolk-shell structure could be explained by the localized "inside-out" Ostwald ripening process, which has been observed in other systems.[15,36] Specifically, VO_2 is generated in the current solvothermal system and then deposited onto the hydrophilic surface of carbon spheres. The initially formed VO_2

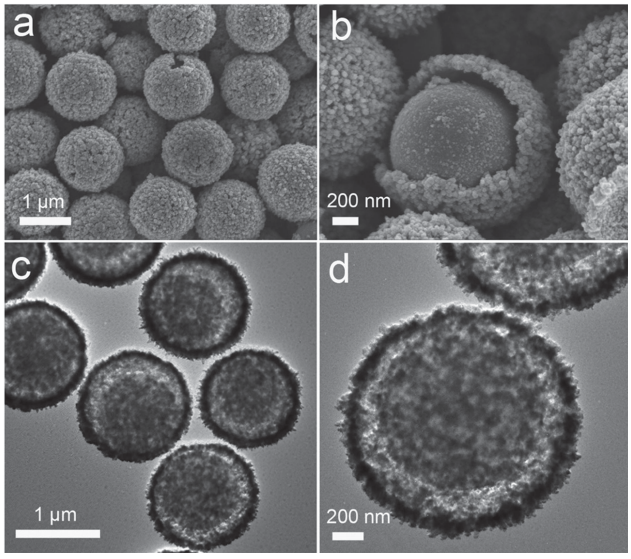

Figure 3. a,b) FESEM and c,d) TEM images of the yolk-shell CS@V-II composite microspheres solvothermally prepared with additional water in the IPA solvent.

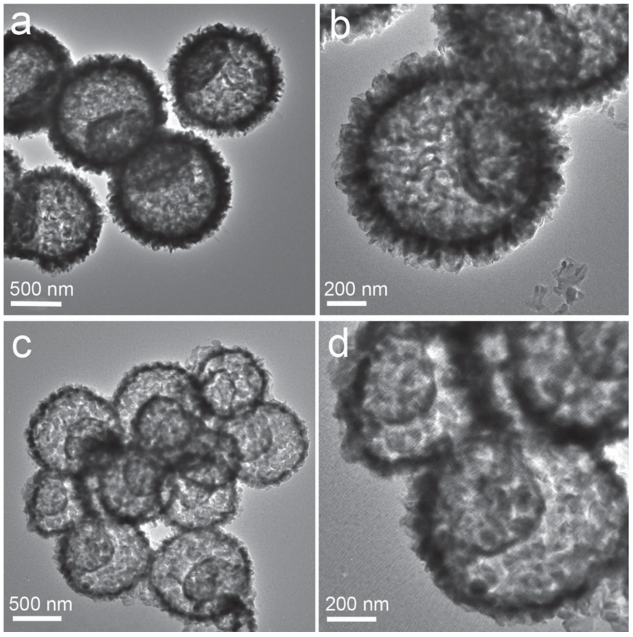

Figure 4. TEM images of the rattle-type V_2O_5 hollow microspheres with a,b) ellipsoidal interior cores and c,d) spherical interior cores prepared by annealing the CS@V-I and CS@V-II microspheres, respectively, in air at 350 °C for 2 h. The heating rate is 3 °C min^{-1}.

on the carbon spheres is likely of low crystallinity or in amorphous state, and tends to dissolve and recrystallize into nanoparticles on the outer surface of the composite microspheres. As the "inside-out" Ostwald ripening proceeds, a polycrystalline shell and a well-defined gap are finally generated.

The as-prepared CS@V microspheres are converted into orthorhombic phase of V_2O_5 (space group: *Pmmn (59)*, a = 11.516 Å, b = 3.566 Å, c = 3.777 Å, JCPDS card no. 41-1426) after calcination in air at 350 °C for 2 h as confirmed by XRD analysis (Figure S3, Supporting Information).[21,22] Then the morphology and structure of V_2O_5 products obtained from annealing the CS@V microspheres with a ramping rate of 3 °C min^{-1} are examined. FESEM images (Figure S4a,b, Supporting Information) show that the product produced from the CS@V-I microspheres well retains the spherical structure, whereas the nanosheet subunits become much thicker. For the V_2O_5 microspheres derived from the CS@V-II microspheres, the primary nanoparticles that construct the shell grow larger after the heat treatment (Figure S4c, Supporting Information). The exterior morphologies of these two types of V_2O_5 microspheres become quite similar, in spite of the distinct morphology and crystal phase of their CS@V precursors. Interestingly, a spherical core is clearly observed inside a broken sphere (Figure S4d, Supporting Information), which implies the complex hollow structure of the as-prepared V_2O_5 microspheres. TEM images as given in **Figure 4** intuitively illustrate the hollow structure of the V_2O_5 microspheres. The V_2O_5 hollow microspheres derived from CS@V-I microspheres possess thicker shells compared to that derived from the CS@V-II microspheres. The hierarchical shell with thick nanosheets of the V_2O_5 hollow microspheres derived from the CS@V-I sample is better elucidated by the magnified TEM image (Figure S5, see Supporting Information). Large cavities are observed in all these V_2O_5 microspheres due to the removal of carbon templates. However, additional particles evidently exist inside the microspheres. For the V_2O_5 hollow microspheres derived from the CS@V-I microspheres, a small ellipsoidal hollow particle can be seen inside each microsphere and it is attached to the outer shell (Figure 4a,b), creating the hollow-in-hollow structure. The interior hollow particles in the V_2O_5 microspheres derived from the CS@V-II microspheres appear to be more spherical and slightly larger (Figure 4c,d).

Removing the hard template from a simple core–shell structure commonly results in single-shelled hollow particles.[2] The formation of complex hollow structures from a simple templating process, such as the rattle-type hollow structure obtained in the present study, is thus considered quite unusual.[37] We postulate that some vanadium species are strongly bonded to the surface of the carbon spheres due to the existence of abundant functional groups, which is supported by the rougher surface of the cores in the CS@V-II microspheres compared with that of the pristine carbon spheres (see Supporting Information Figure S1 and Figure 3b). During the annealing process, the outer layer of vanadium precursor crystallizes into the rigid V_2O_5 outer shell, which is similar to typical template-assisted formation of hollow structures. Meanwhile, the vanadium species bonded on the surface of carbon spheres first shrink into smaller core due to the gradual removal of the carbonaceous species, and finally form the small interior hollow particles upon complete elimination of the carbon template. Thus the rattle-type hollow structure with an additional interior hollow core is generated.

The interior structure of the V_2O_5 hollow microspheres is also greatly determined by the heating rate and the temperature of the annealing process. **Figure 5** shows the FESEM and TEM images of the V_2O_5 microspheres obtained by annealing

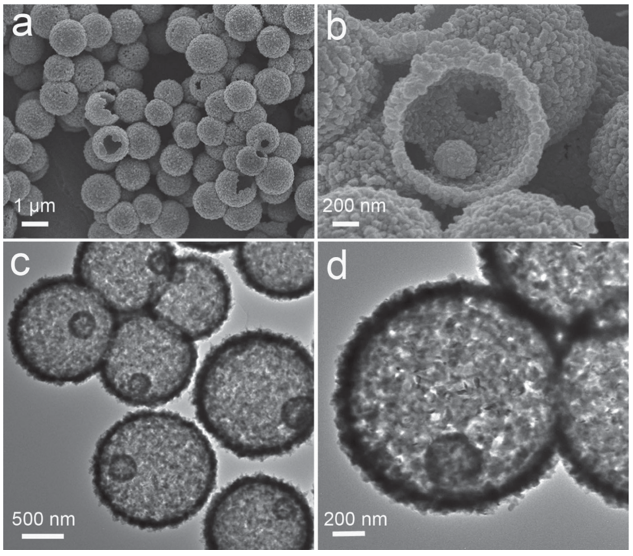

Figure 5. a,b) FESEM and c,d) TEM images of rattle-type V_2O_5 hollow microspheres obtained by annealing the yolk-shell CS@V-II microspheres in air at 350 °C for 2 h with a heating rate of 1 °C min^{-1}.

the CS@V-II microsphere in air at 350 °C with a slow ramping rate of 1 °C min^{-1}. As shown in Figure 5a, the exterior morphology of the V_2O_5 microspheres is similar to that of the previous sample prepared with a higher heating rate. A relatively compact outer shell formed by nanoparticles is revealed by the magnified TEM image (Figure S6, Supporting Information). The FESEM image of a broken microsphere (Figure 5b) demonstrates the yolk-shell structure with a small spherical core. Such a structure is further confirmed by the corresponding TEM image (Figure 5c,d). The lower contrast in the center region of the core suggests its hollow structure. However, the interior core is much smaller than that in the rattle-type V_2O_5 hollow microspheres prepared from the same precursor but with a higher ramping rate of 3 °C min^{-1}. Further increasing the anneal temperature to 400 °C results in the disappearance of the interior core. As shown in Figure S7 (see Supporting Information), the sample consists of single-shell microspheres with a shell thickness of around 100 nm. Moreover, the shell becomes more open with many large pores. Hence the hollow structure of the V_2O_5 microspheres could be easily tuned by varying the annealing conditions.

The V_2O_5 hollow microspheres synthesized in this work are attractive as cathode materials for lithium-ion batteries. As a demonstration, here we investigate the electrochemical properties of the V_2O_5 hollow microspheres shown in Figure 5. **Figure 6**a depicts the discharge and charge curves for the 1st, 2nd, 10th, 30th, 50th and 100th cycles, which are obtained at a constant current density of 300 mA g^{-1} in the voltage range of 2–4 V vs. Li/Li^+. The three plateaus observed in the discharge curves at 3.3, 3.1, and 2.2 V indicate the multi-step Li^+ ion insertion process, which correspond to the phase changes from α-V_2O_5 to ε-$Li_{0.5}V_2O_5$, then to δ-LiV_2O_5 and finally to γ-$Li_2V_2O_5$, respectively.[26,38] The observed plateaus at 2.60, 3.27, and 3.46 V in the charge curves correspond to the lithium de-intercalation process and the successive reverse phase transformation from γ-$Li_2V_2O_5$

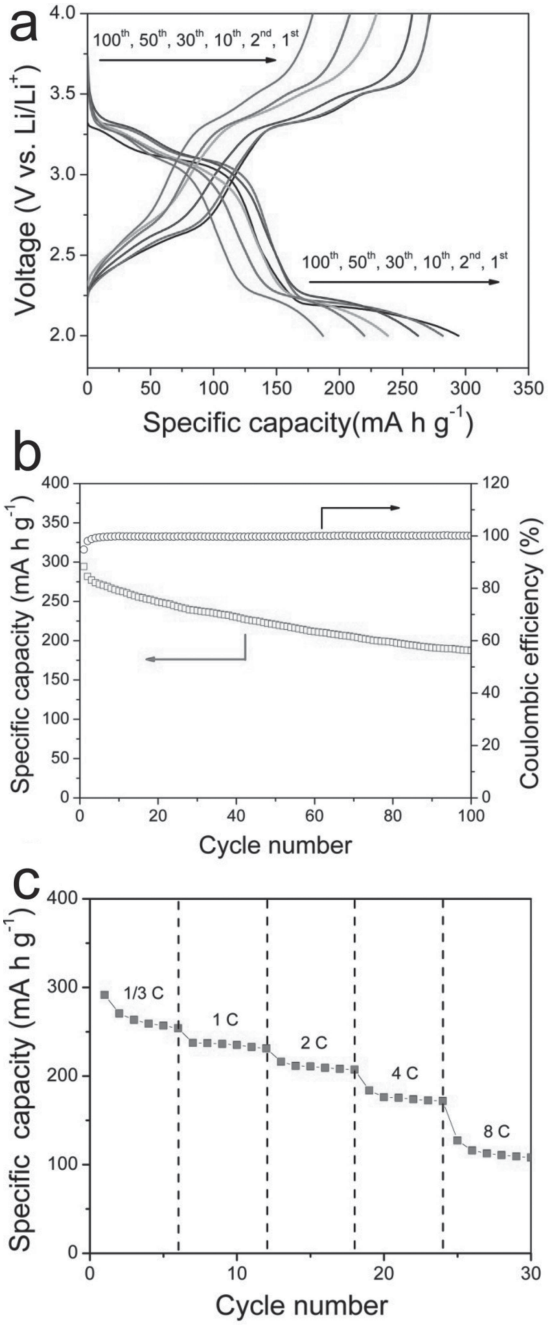

Figure 6. a) Discharge/charge voltage profiles of the rattle-type V_2O_5 hollow microspheres in the voltage range of 2–4 V vs. Li/Li^+ at a current density of 300 mA g^{-1}; b) cycling performance and Coulombic efficiency of the electrode at a current density of 300 mA g^{-1}; c) rate performance of the electrode in the voltage range of 2–4 V vs. Li/Li^+. Here 1 C = 300 mA g^{-1}.

to δ-LiV_2O_5, then to ε-$Li_{0.5}V_2O_5$, and to α-V_2O_5 respectively.[39] A high initial discharge capacity of 290 mA h g^{-1} is obtained within the voltage range of 2–4 V, which is very close to the theoretical capacity (294 mA h g^{-1}). As can be seen from Figure 6a, the discharge and charge plateaus are generally remain stable over the repeated cycles, which indicate the good structural reversibility

of the V_2O_5 hollow microspheres. Figure 6b plots the specific discharge capacity and corresponding Coulombic efficiency as a function of cycle number at a constant current density of 300 mA g^{-1}. The sample exhibits good capacity retention upon prolonged cycling with high Coulombic efficiency close to 100%. It still retains a specific discharge capacity of 220 and 187 mA h g^{-1} at the 50th, 100th cycles, respectively. The average capacity fading rate is 0.35% per cycle. As a comparison, the cycling performance of the V_2O_5 single-shell hollow microspheres is given in Supporting Information Figure S8. The sample delivers lower specific capacity under the identical testing conditions, which might suggest the lower utilization of active materials compared with the rattle-type structure. Figure 6c shows the rate performance of the V_2O_5 hollow microspheres in the voltage range of 2–4 V. An initial discharge capacity of 291 mA h g^{-1} is obtained at a low current density of 1/3 C (100 mA g^{-1}), which stabilizes at around 254 mA h g^{-1} after 6 cycles. It delivers specific discharge capacities of 237, 216, 183, and 127 mA h g^{-1} at 1 C (300 mA g^{-1}), 2 C, 4 C and 8 C, respectively. The electrochemical performance is quite impressive, and shows certain improvement when comparing with some previous reports, such as V_2O_5 nanoparticles,[40] nanorods,[38,41] and porous or hollow spheres.[28,29] The enhanced electrochemical performance of such V_2O_5 hollow microspheres might be related to the novel hollow structure of the microspheres in several aspects. First, the nanometer scale thickness of both the interior and exterior shells would shorten the Li^+ ion diffusion and electron transport distance. Second, the porous shells and the void space within the hollow microspheres ensure the efficient electrolyte penetration and increase the contact area between the electrode and electrolyte. Furthermore, the micrometer size particles might provide good structural integrity of the electrode and prevent aggregation of primary nanoparticles.

3. Conclusions

In summary, novel rattle-type V_2O_5 hollow microspheres with different shell structures are successfully synthesized with the assistance of carbon colloidal spheres as hard templates. Carbon spheres@vanadium-precursor (CS@V) core–shell composite microspheres with various morphologies and structures are first prepared through a facile solvothermal method. V_2O_5 hollow microspheres with various shell architectures can be obtained after removing the carbon microspheres by calcination in air. Moreover, the interior hollow shell can be tailored by varying the temperature ramping rate and calcination temperature. When evaluated as a cathode material for lithium-ion batteries, the rattle-type V_2O_5 hollow microspheres exhibit enhanced cycling stability and rate capability. The remarkable electrochemical performance could be ascribed to the unique hollow structure that facilitates the electronic/ionic transport and provides good structural stability.

4. Experimental Section

Materials Synthesis: The carbon spheres (CS) were hydrothermally synthesized according to the method in an early report.[34] To prepare the CS@V-I composite microspheres, 50 mg of as-prepared carbon spheres was dispersed in 30 mL of isopropanol (IPA) by ultrasonication, followed by addition of 0.2 mL of vanadium oxytriisopropoxide (VOT). The as-obtained mixture was sealed in a Teflon-lined autoclave and solvothermally treated at 200 °C for 12 h. To prepare the CS@V-II composite microspheres, 2 mL of deionized (DI) water was added into the above mixture while keeping other parameters unaltered.

The V_2O_5 hollow microspheres with various interior structures can be obtained by annealing the solvothermal products in air. The rattle-type V_2O_5 hollow microspheres were obtained by annealing the CS@V precursors in air at 350 °C for 2 h, with a ramping rate of 3 or 1 °C min^{-1}. Single-shelled V_2O_5 hollow microspheres were prepared after annealing in air at 400 °C for 2 h using a ramping rate of 1 °C min^{-1}.

Materials Characterization: Crystallographic phases of all the products were investigated by powder X-ray diffraction (Bruker, D8-Advance XRD, Cu Kα, λ = 1.5406 Å). Morphologies of the samples were examined by field-emission scanning electron microscope (FESEM; JEOL, JEM-6700F, 5 kV) and transmission electron microscope (TEM; JEOL, JEM-2010, 200 kV).

Electrochemical Measurements: The working electrode slurry was prepared by dispersing V_2O_5, carbon black (Super-P-Li) and poly(vinylidene fluoride) (PVDF) binder in *N*-methylpyrrolidone with a weight ratio of 70:20:10. The slurry was spread on aluminum foil disks and dried in a vacuum oven at 120 °C overnight prior to Swagelok-type cells assembly. Lithium foil was used as the counter and reference electrode, and 1.0 M $LiPF_6$ in ethyl carbonate/dimethyl carbonate (1:1 v/v ratio) was used as the electrolyte. Galvanostatic charging/discharging tests were conducted on a battery tester (NEWAER).

Supporting Information

Supporting Information is available from the Wiley Online Library or from the author.

Received: March 19, 2013
Revised: April 26, 2013
Published online: May 31, 2013

[1] X. W. Lou, L. A. Archer, Z. C. Yang, *Adv. Mater.* **2008**, *20*, 3987.
[2] F. Caruso, *Chem. Euro. J.* **2000**, *6*, 413.
[3] S. W. Kim, M. Kim, W. Y. Lee, T. Hyeon, *J. Am. Chem. Soc.* **2002**, *124*, 7642.
[4] J. Hu, M. Chen, X. Fang, L. Wu, *Chem. Soc. Rev.* **2011**, *40*, 5472.
[5] X. Lai, J. E. Halpert, D. Wang, *Energy Environ. Sci.* **2012**, *5*, 5604.
[6] J. F. Chen, H. M. Ding, J. X. Wang, L. Shao, *Biomaterials* **2004**, *25*, 723.
[7] C. Qi, Y. J. Zhu, B. Q. Lu, X. Y. Zhao, J. Zhao, F. Chen, *J. Mater. Chem.* **2012**, *22*, 22642.
[8] J. H. Pan, X. W. Zhang, A. J. Du, D. D. Sun, J. O. Leckie, *J. Am. Chem. Soc.* **2008**, *130*, 11256.
[9] Y. H. Ng, S. Ikeda, T. Harada, S. Higashida, T. Sakata, H. Mori, M. Matsumura, *Adv. Mater.* **2007**, *19*, 597.
[10] H. J. Koo, Y. J. Kim, Y. H. Lee, W. I. Lee, K. Kim, N. G. Park, *Adv. Mater.* **2008**, *20*, 195.
[11] J. F. Qian, P. Liu, Y. Xiao, Y. Jiang, Y. L. Cao, X. P. Ai, H. X. Yang, *Adv. Mater.* **2009**, *21*, 3663.
[12] W. Y. Li, L. N. Xu, J. Chen, *Adv. Funct. Mater.* **2005**, *15*, 851.
[13] H. G. Zhang, Q. S. Zhu, Y. Zhang, Y. Wang, L. Zhao, B. Yu, *Adv. Funct. Mater.* **2007**, *17*, 2766.
[14] X. W. Lou, D. Deng, J. Y. Lee, L. A. Archer, *Chem. Mater.* **2008**, *20*, 6562.
[15] X. W. Lou, Y. Wang, C. L. Yuan, J. Y. Lee, L. A. Archer, *Adv. Mater.* **2006**, *18*, 2325.

[16] J. J. Teo, Y. Chang, H. C. Zeng, *Langmuir* **2006**, *22*, 7369.
[17] H. G. Yu, J. G. Yu, S. W. Liu, S. Mann, *Chem. Mater.* **2007**, *19*, 4327.
[18] X. W. Lou, C. M. Li, L. A. Archer, *Adv. Mater.* **2009**, *21*, 2536.
[19] X. W. Lou, C. L. Yuan, L. A. Archer, *Adv. Mater.* **2007**, *19*, 3328.
[20] J. Liu, S. Z. Qiao, J. S. Chen, X. W. Lou, X. R. Xing, G. Q. Lu, *Chem. Commun.* **2011**, *47*, 12578.
[21] A. Q. Pan, J. G. Zhang, Z. M. Nie, G. Z. Cao, B. W. Arey, G. S. Li, S. Q. Liang, J. Liu, *J. Mater. Chem.* **2010**, *20*, 9193.
[22] A. M. Cao, J. S. Hu, H. P. Liang, L. J. Wan, *Angew. Chem. Int. Ed.* **2005**, *44*, 4391.
[23] J. Liu, H. Xia, D. F. Xue, L. Lu, *J. Am. Chem. Soc.* **2009**, *131*, 12086.
[24] Y. Wang, G. Z. Cao, *Adv. Mater.* **2008**, *20*, 2251.
[25] A. Q. Pan, H. B. Wu, L. Yu, T. Zhu, X. W. Lou, *ACS Appl. Mater. Interfaces* **2012**, *4*, 3874.
[26] Y. S. Hu, X. Liu, J. O. Muller, R. Schlogl, J. Maier, D. S. Su, *Angew. Chem. Int. Ed.* **2009**, *48*, 210.
[27] D. M. Yu, C. G. Chen, S. H. Xie, Y. Y. Liu, K. Park, X. Y. Zhou, Q. F. Zhang, J. Y. Li, G. Z. Cao, *Energy Environ. Sci.* **2011**, *4*, 858.
[28] S. Q. Wang, S. R. Li, Y. Sun, X. Y. Feng, C. H. Chen, *Energy Environ. Sci.* **2011**, *4*, 2854.
[29] S. Q. Wang, Z. D. Lu, D. Wang, C. G. Li, C. H. Chen, Y. D. Yin, *J. Mater. Chem.* **2011**, *21*, 6365.
[30] A. Q. Pan, T. Zhu, H. B. Wu, X. W. Lou, *Chem. Euro. J.* **2013**, *19*, 494.
[31] A. Q. Pan, H. B. Wu, L. Yu, X. W. Lou, *Angew. Chem. Int. Ed.* **2013**, *52*, 2226.
[32] M. Sasidharan, N. Gunawardhana, M. Yoshio, K. Nakashima, *J. Electrochem. Soc.* **2012**, *159*, A618.
[33] C. Wu, X. Zhang, B. Ning, J. Yang, Y. Xie, *Inorg. Chem.* **2009**, *48*, 6044.
[34] X. M. Sun, Y. D. Li, *Angew. Chem. Int. Ed.* **2004**, *43*, 597.
[35] G. Q. Zhang, L. Yu, H. E. Hoster, X. W. Lou, *Nanoscale* **2013**, *5*, 877.
[36] J. S. Chen, C. M. Li, W. W. Zhou, Q. Y. Yan, L. A. Archer, X. W. Lou, *Nanoscale* **2009**, *1*, 280.
[37] X. Lai, J. Li, B. A. Korgel, Z. Dong, Z. Li, F. Su, J. Du, D. Wang, *Angew. Chem. Int. Ed.* **2011**, *50*, 2738.
[38] S. L. Chou, J. Z. Wang, J. Z. Sun, D. Wexler, M. Forsyth, H. K. Liu, D. R. MacFarlane, S. X. Dou, *Chem. Mater.* **2008**, *20*, 7044.
[39] X. F. Zhang, K. X. Wang, X. Wei, J. S. Chen, *Chem. Mater.* **2011**, *23*, 5290.
[40] S. H. Ng, T. J. Patey, R. Buechel, F. Krumeich, J. Z. Wang, H. K. Liu, S. E. Pratsinis, P. Novak, *Phys. Chem. Chem. Phys.* **2009**, *11*, 3748.
[41] K. Takahashi, Y. Wang, G. Z. Cao, *Appl. Phys. Lett.* **2005**, *86*, 053102.